The Microrheology of Red Blood Cell Suspensions

HARRY L. GOLDSMITH

From the McGill University Medical Clinic, The Montreal General Hospital, Montreal 25, Quebec, Canada

ABSTRACT The general problem of microrheology is to predict the macroscopic flow properties of a material from a detailed description of the behavior of its constituent elements. This approach has been used to study suspensions of human red cells in plasma or Ringer's solution flowing steadily in rigid tubes 8–25 times the red cell diameter by observing individual cell motions under the microscope. The results have been compared with those previously obtained with model particles under similar conditions. In very dilute suspensions single red cells rotated in orbits similar to those of rigid discs at low flow rates, but, in common with model deformable particles, were observed to migrate away from the tube wall. Linear rouleaux of red cells rotated as rodlike particles and were flexible, bending during their rotational orbits in a manner similar to that of filaments of nylon or Dacron. Transparent concentrated suspensions were produced by preparing ghost cells reconstituted in biconcave form in plasma. In these, the motions of some unhemolyzed red cells were followed. The erythrocyte velocity profiles were blunted at concentrations above 20%; the cell paths were erratic because of frequent radial displacements, especially at the tube periphery, with the particles being markedly deformed and oriented parallel to the flow. Finally, the difference in flow pattern in large and small vessels is discussed and some relevant model experiments are described.

To the rheologist, vertebrate blood is a very concentrated suspension of deformable, disclike particles which circulates in distensible vessels whose sizes range from less than 1 to 3000 red cell diameters. As shown by measurements of the viscosity, blood possesses a remarkable fluidity when compared to other model particle suspensions of spheres and discs. This appears to be due in large measure to the deformability of the red cell, which has been seen to change shape during flow in the capillaries (1, 2) and, as described below, to deform also in large vessels owing to collisions with neighboring particles (3).

Fig. 1 compares the relative viscosity, η_r (viscosity of suspension/viscosity of pure suspending phase), of a number of model dispersions with that of blood as a function of the volume concentration, c, of suspended particles. It is evi-

dent that at any given c, η_r is considerably lower in the case of mammalian blood. Thus, Müller (10) found that rubber discs of axis ratio (thickness/diameter) = 0.18 in aqueous glycerol would only flow with great difficulty at 30% concentration in a rigid tube 5 times the diameter of the discs. Even at $c = 0.8$, the relative viscosity of the dog's blood shown in Fig. 1 is still only about 11 (4), whereas in suspensions of rigid spheres (5, 6) and discs $\eta_r > 200$ when c is only 0.45. If the deformability of the red cell is responsible for the

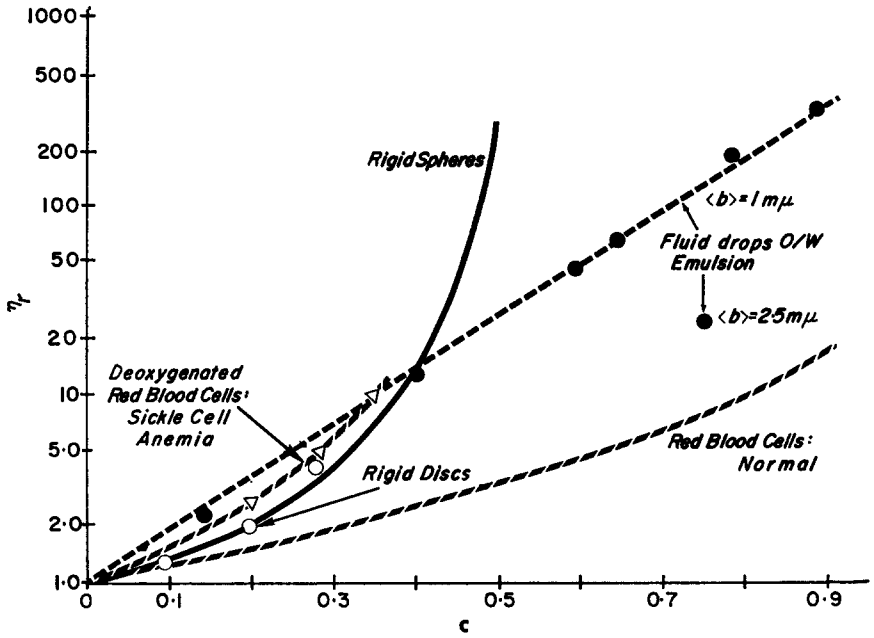

FIGURE 1. The relative viscosity of a normal dog red blood cell suspension [from the data of Bayliss (4)] as a function of volume concentration, compared with that of suspensions of small, rigid, spherical latex particles (5, 6), an emulsion of oil droplets in water (O/W) (7) (●), and rigid rubber discs in glycerol (○). Also shown are points obtained with sickled red blood cells (8) (△), demonstrating the effect of shape and rigidity. *Figure reprinted by permission from Rheology: Theory and Applications* (IV), *Academic Press, Inc., New York, 1967.*

relative ease of blood flow, its viscosity should be compared to that of emulsions of deformable droplets. However, as Fig. 1 shows, η_r for oil-in-water emulsions having a mean droplet radius of 1–2.5 μ (7) is appreciably greater than that of blood at all c. A packed column of erythrocytes in a centrifuge tube containing less than 3% of trapped plasma never reaches the quasi-solid consistency of oliomargarine found with emulsions already at 75% concentration.

However, when the cells lose both their shape and deformability, as in sickle-cell anemia, the relative viscosity increases drastically (8, 11), η_r being

higher than that for rigid spheres. Similar results have been obtained for cells hardened with formalin, acetaldehyde, or tannic acid, which did not lose their shape (12, 13).

These observations of the over-all flow properties of whole blood and model particle dispersions cannot be explained without first understanding the flow behavior of the constituent elements of the suspensions. This is the approach of microrheology which has as its general problem the prediction of the macroscopic flow properties of a material from a detailed description of the behavior of the elements of which it is composed (9). Here, our materials are suspensions of human red blood cells in plasma or Ringer's solution, and the elements are the elementary volumes of fluid each containing an erythrocyte. The behavior of these elements when undergoing steady flow in cylindrical tubes, first in isolation from each other at great dilution, and then when interacting at progressively increasing concentrations, as seen under the microscope, will be described.

The techniques used to follow red cell behavior were adapted from an extensive study of the microrheology of dispersions of model rigid and deformable spheres and cylinders (9) undergoing tube flow over a range of the Reynolds number, Re, from 10^{-3} to 10:

$$\mathrm{Re} = \frac{R\bar{u}\rho}{\eta}$$

R being the tube radius, $\bar{u}$ the mean linear velocity, and ρ and η the respective density and viscosity of the suspending liquid. It will be shown that some of the phenomena described below for red cells have previously been observed in the model studies, and there analyzed in terms of rigorous hydrodynamic theory. This has greatly facilitated the investigation of the microscopic flow properties of red cells.

Most of the results with erythrocytes have been obtained in tubes whose diameters ranged from 65 to 200 μ, i.e. large compared to the red cell and thus applicable only to flow in small arteries and veins. However, it must be emphasized that the flow regime in the capillaries of the microcirculation, which are of the same size or smaller than the red cell, is quite different and will therefore be separately treated below.

TUBES LARGE COMPARED TO RED CELLS

Dilute Suspensions

ROTATION To understand red cell behavior in tube flow, it is necessary to describe briefly what is known about the motions of single model particles under similar conditions, as schematically illustrated in Fig. 2. The figure represents Poiseuille flow of a Newtonian liquid as seen in the median or

diametrical plane of a rigid tube of radius R. The fluid velocity $u(r)$ in the x or axial direction increases parabolically from zero at the wall, with decreasing radial distance r, to a maximum at the center, according to the equation

$$u(r) = \frac{2Q}{\pi R^4}(R^2 - r^2) = u(0)\left[1 - \frac{r^2}{R^2}\right] \quad (1)$$

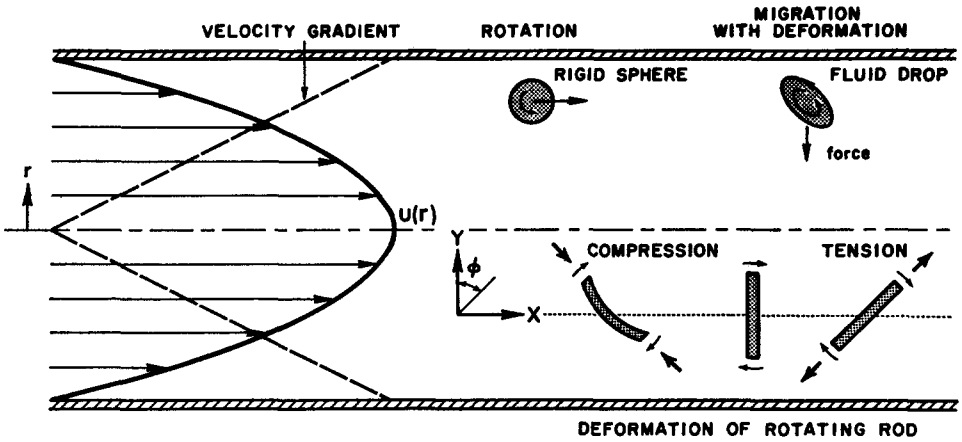

FIGURE 2. Schematic representation of the behavior of model particles suspended in a liquid subject to Poiseuille flow. The diagram shows the median plane of the tube with the parabolic velocity distribution, $u(r)$, of the flow in the x direction, and the linear variation of the velocity gradient with the radial distance, r, from the axis. The stresses in the fluid cause a rigid sphere to rotate, and a fluid drop to deform into an ellipsoid which migrates away from the wall. The same stresses, tensile and compressive, in alternate quadrants of the angle ϕ, produce buckling of a rotating flexible rod. *Figure reprinted by permission from Federation Proceedings, 1967, 26:1813.*

Q being the volume flow rate and $u(0)$ the center-line fluid velocity. The gradient in velocity or shear rate, G, which increases with r according to the relation

$$G(r) = \frac{du}{dr} = \frac{4Q}{\pi R^4} r \quad (2)$$

gives rise to fluid stresses which exert a torque on the surface of suspended particles and cause them to rotate. A small rigid sphere rotates with uniform angular velocity = $G/2$ (9). The case of a rigid spheroid, either oblate (saucer-shaped) or prolate (cigar-shaped), in a simple shear flow was treated by Jeffery (14), who calculated the motion of the axis of revolution (Fig. 3) and found it to be somewhat like that of a precessing top. The angular velocity

$d\phi/dt$, ϕ being the angle of the axis of revolution with the Y-axis as shown in Figs. 2 and 3, is now variable and given by

$$\frac{d\phi}{dt} = \frac{G}{r_p^2 + 1}(r_p^2 \cos^2 \phi + \sin^2 \phi) \tag{3}$$

r_p is the axis ratio axis of revolution/diametrical axis of the spheroid (<1 for oblate or disclike particles, >1 for prolate or rodlike particles). Experiments have shown (9, 15) that the theory applies also to small rigid discs and rods in Poiseuille flow provided that r_p is replaced by r_e, an experimentally deter-

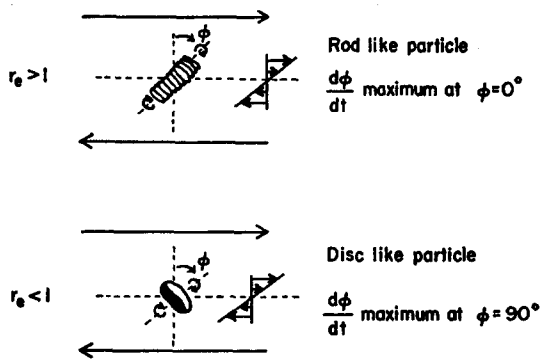

FIGURE 3. Diagram illustrating the variation in angular velocity of spheroids in Poiseuille flow according to the theory of Jeffery (14). In dilute heparinized plasma suspensions, both disclike (single cells) and rodlike (rouleaux) particles may be seen at low flow rates. The tube (not shown) is considered as moving with a velocity equal and opposite to that of the cell, so that the particle is at the origin of the flow field; i.e. liquid moves to the right, above it, and to the left, below it.

mined axis ratio representing the spheroid which has the same period of rotation, T, as the cylindrical particle:

$$T = \frac{2\pi}{G}\left(r_e + \frac{1}{r_e}\right) \tag{4}$$

As schematically shown in Fig. 3, equation 3 predicts that the angular velocities of rod- and disclike particles are a maximum when the particle major axis lies across the direction of flow, and minimum but not zero when aligned with the flow.

Studies of human red cells in heparinized plasma were made by following the particles at $c < 0.02$ down polypropylene or glass tubes (3, 16) at mean linear velocities $\bar{u}$ from 0.5 to 10 tube diameters/sec [wall velocity gradients or shear rates $G(R) = 4\bar{u}/R$, assuming Poiseuille flow, from 1 to 20 sec^{-1}]. The results obtained from the analysis of movie film of the cell motions showed that the above theory applies to single erythrocytes and to straight-chain

rouleaux from two to 20 cells. The mean value of r_e calculated from equation 4 was found to be 0.40 for a single cell, increasing for two- and three-cell rouleaux, and reaching 1.0 for four-cell linear aggregates whose length was approximately equal to their diameter and which rotated with almost uniform angular velocity.

As a result of the erythrocyte's periodic angular motion, the particle spends more of its time aligned with the flow than across it. Thus, measurements of

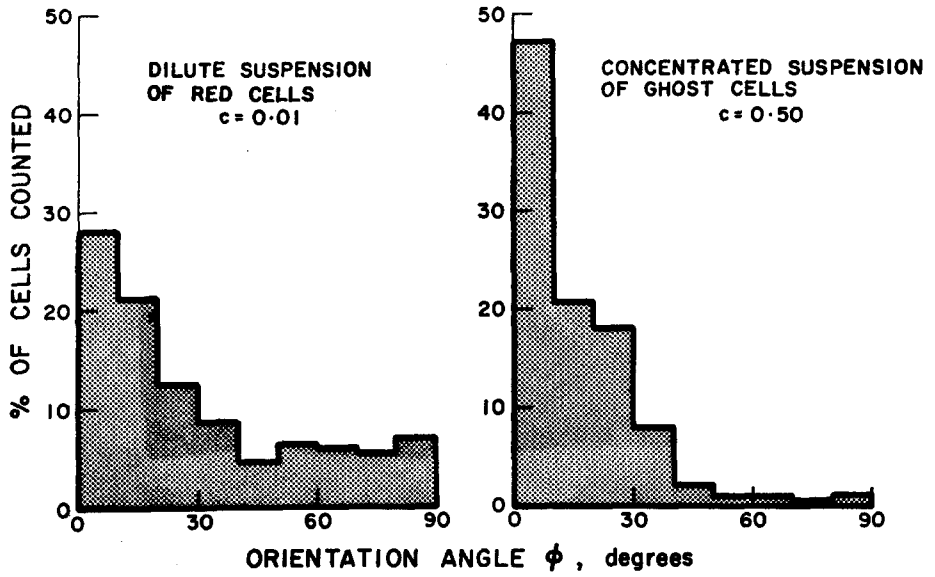

FIGURE 4. The differential steady-state distribution of human red blood cells with respect to the angle ϕ in a dilute 1% plasma suspension (left) and in a concentrated 50% ghost cell suspension (right) undergoing flow in a tube, $R = 35\ \mu$. The results, obtained by analysis of photomicrographs of cells in the tube, show a much greater alignment of particles with the flow (ϕ close to 0°) in the concentrated suspension. Although the particle rotates through an angle of 180° in each half-orbit (cf. Figs. 5 and 12), the numbers of cells at equivalent angles in each quadrant were added together in the drawing.

the steady-state differential distribution in ϕ, $p(\phi)$, of erythrocytes in Ringer's solution (where rouleaux formation is suppressed) in the tube shown in the left-hand panel of Fig. 4 indicate that 49% of the cells counted have orientations $\phi = 0° \pm 20°$, whereas, if the distribution were random, 22% of the cells would be in this orientation. A value of $p(\phi)$ can be calculated by assuming the particle rotation to obey equation 3 and from the steady-state condition

$$p(\phi)\frac{d\phi}{dt} = \text{constant}$$

By substituting $d\phi/dt$ from equation 3 and evaluating the constant from the condition $\int_0^{2\pi} p(\phi)\, d\phi = 1$, one obtains (17)

$$p(\phi) = \frac{r_e}{2\pi(r_e^2 \cos^2\phi + \sin^2\phi)} \tag{5}$$

and, for the integral distribution function $P(\phi)$,

$$P(\phi) = \frac{1}{2\pi} \tan^{-1}\left(\frac{\tan\phi}{r_e}\right) \tag{6}$$

According to equation 6, for a disclike particle having $r_e = 0.40$, $P(20) = 0.47$, close to the experimental value of 0.49 found at low flow rates [$G(R) < 20\ \text{sec}^{-1}$], where the cells' behavior is similar to that of rigid discs.

Rouleaux consisting of five or more cells in linear array rotated as prolate spheroids, i.e. with $d\phi/dt$ maximum when $\phi = 0°$, as illustrated in Fig. 5*A*, and with $r_e > 1$. They were, however, subject to bending while rotating, as discussed below.

DEFORMATION AND MIGRATION The stresses in the fluid undergoing Poiseuille flow also bring about deformation of liquid drops and flexible rods (see Fig. 2). In the case of a liquid drop suspended in another immiscible phase, the tangential fluid stresses are transmitted into the particle interior and set up a system of velocity gradients inside the drop by internal circulation (18, 19). The normal stresses, which as shown in Fig. 2 are compressive and tensile in alternate quadrants, lead to deformation of the drop into a prolate ellipsoid in which the stresses are balanced by the interfacial tension γ (20). In a given system, increasing the velocity gradient leads to increasing deformation and ultimately to breakup of the drop in a manner which depends on the ratio λ = drop viscosity/suspending fluid viscosity (20, 21), as is illustrated in Fig. 6. The equation given by Taylor (20) for the deformation of a drop of radius b into an ellipsoid of length L and breadth B is

$$D = \frac{L - B}{L + B} = \frac{Gb\eta}{\gamma} \frac{(19\lambda + 16)}{(16\lambda + 16)} \tag{7}$$

An important result of drop deformation in the tube has been shown to be the migration away from the wall. At very low Reynolds number and small particle/tube size ratios, both experiment (15) and theory (9, 22) indicate that there is no net force tending to propel a *rigid* particle away from the wall to the tube axis. However, a deformed drop under these conditions migrates axially at a rate, $-dr/dt$, which increases with increasing particle size, velocity gradient (and hence deformation), and radial distance from the tube axis. This effect has been attributed (22) to the drop deformation, which brings

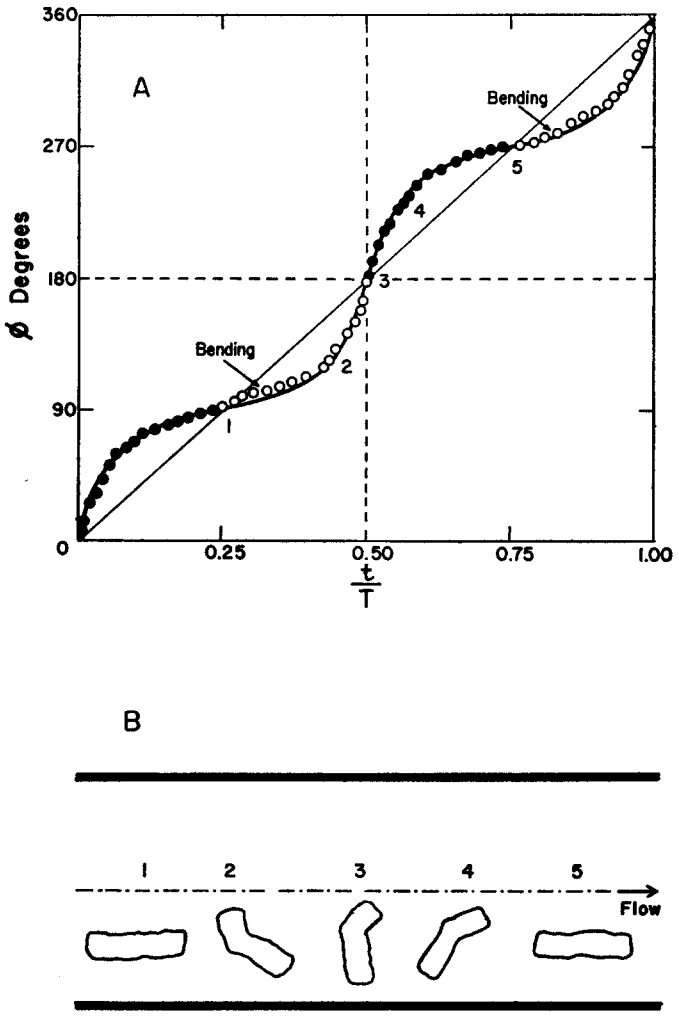

FIGURE 5. The upper part shows the variation in the ϕ-orientation of a 15 cell rouleau in Poiseuille flow. The points are experimental, and the line is calculated from equation 3 for the measured value of $r_e = 2.9$ for this particle. The lower part shows the rouleau bending in alternate quadrants, where the fluid stresses are compressive (cf. Fig. 2). *Figure reprinted by permission from Science, 1966, 153:1406.*

about an additional perturbation in the flow around the particle from that which exists around a sphere; this, when reflected off the wall, yields an inwardly directed force. The migration velocity resulting from this force in Poiseuille flow was calculated to be (22)

$$-\frac{dr}{dt} = \frac{G^2 b^4 \eta}{\gamma(R-r)^2} \cdot \frac{33(54\lambda^2 + 102\lambda + 54)(19\lambda + 16)}{4480(\lambda + 1)^3} \qquad (8)$$

According to equation 8, the migration rate in a given system should decrease sharply with increasing distance from the wall; thus the predicted dr/dt at a radial position $0.7R$ is only 7% of the value at $0.9R$.

Although deformation of human red blood cells has not been detected in the analysis of the movie films, at wall shear rates of >20 sec^{-1} in tubes having

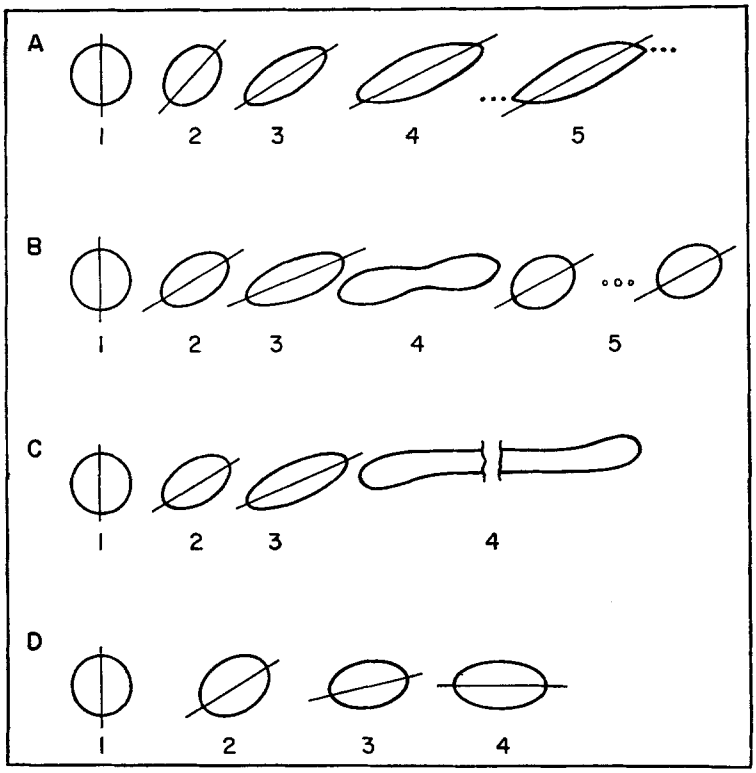

FIGURE 6. The deformation of liquid droplets, initially spherical, suspended in viscous oils subjected to progressively increasing flow (in the direction of the horizontal axis from left to right) in going from 1 to 5. *A*. A water drop in silicone oil (λ effectively zero) deforms into an ellipsoid whose eccentricity increases until it breaks up by spitting out tiny drops. *B* and *C*. Oil-in-oil systems in which $\lambda \sim 1$ and in which breakup occurs by a necking-off process, resulting in satellite drops in *B* and in a very long-drawn-out thread in *C*. *D*. A viscous drop ($\lambda > 10$) in which there is no breakup, only a complete alignment with the flow. *Figure reprinted by permission from the Journal of Colloid Science, 1960, 16:238.*

$R < 40\ \mu$, axial migration, especially near the wall, has been inferred from measurements of the change in cell distribution within the tube with increasing distance from the tube entry (3). An example is given in Fig. 7, illustrating the fact that the cells, after entering the flow tube from a wider reservoir, progressively accumulated in the central portion of the tube.

As a result of the normal stresses in flow, as shown in Fig. 2, a rodlike par-

ticle while rotating is subjected to compressive forces in alternate quadrants, which, if the particle axis ratio or the velocity gradient is sufficiently high, can lead to buckling. The particle will tend straighten out in the subsequent quadrant, where the forces are tensile, such an orbit being described as "springy." This behavior has been observed with nylon, Dacron, and rayon filaments (23) and, more recently, with linear chains of conducting spheres first brought together by application of an electric field and then rotated at low G in the absence of the field (24). Calculations show that the critical value

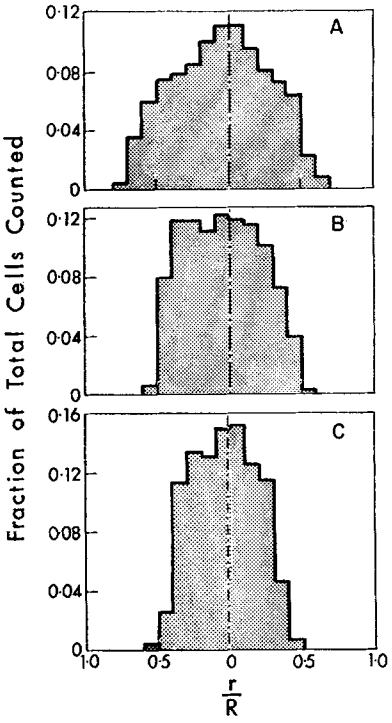

FIGURE 7. Axial migration of human red cells in a 1% Ringer's solution as illustrated by the change in distribution in the median plane with distance down a tube of 75 μ diameter, at $\bar{u}$ = 0.32 cm sec^{-1}. All cells crossing the median plane were counted in a frame-by-frame analysis of the movie film taken at 0.25 cm (A), 2.80 cm (B), and 4.80 cm (C) from the tube entrance. Because of inward migration, the peripheral cell-free layer progressively widens with flow down the tube. *Figure adapted by permission from Federation Proceedings, 1967, 26:1813.*

of the product, Gr_p, at which buckling occurs at the position of maximum compression, $\phi = 45°$, is given by (23)

$$(Gr_p)_{crit} = \frac{E_b(\log_e 2r_e - 1.50)}{2r_p^4} \qquad (9)$$

E_b being the bending modulus of the rod.

Observations made with rouleaux of red cells having 10 or more cells in linear array have demonstrated the existence of springy orbits (3, 16) (Figs. 5B and 8A), but these occur at $(Gr_p)_{crit}$ values only about 10^{-7} of those found for Dacron rods of 8 μ diameter. As with flexible filaments, at a given G, in-

creasing the number of cells in linear array brought an increase in flexibility, so that the ends of the particles became capable of independent movement (Fig. 8*B*). Such orbits, known as snake orbits, were strikingly similar to those

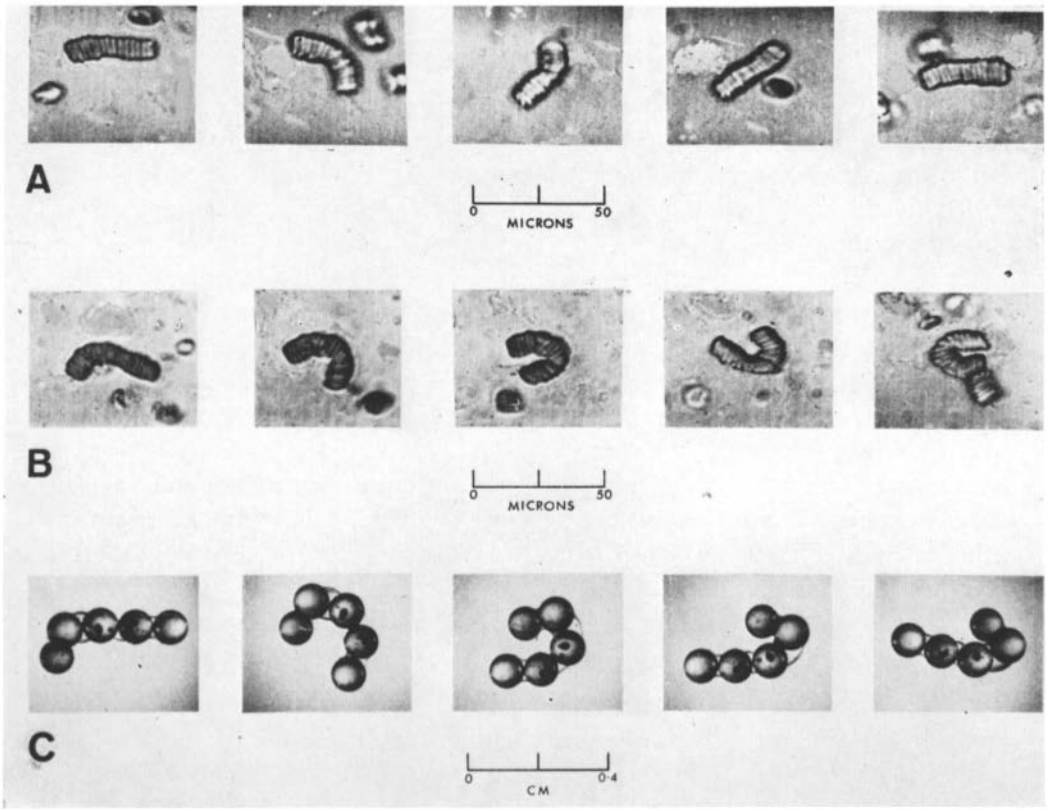

FIGURE 8. Photomicrographs of the bending of rouleaux during clockwise rotation in the flow, from left to right, at $\bar{u} = 0.03$ cm sec^{-1} in a tube of 120 μ diameter. The nearest tube wall, below the particles, is not shown in the photographs. *A*. "Springy" orbit, in which a rouleau of 13 cells buckles in one quadrant and straightens out again in the next. *B*. "Snake" rotation, in which the ends of the particle (20 cells long) are able to bend independently, and which is strikingly similar to *C*, the rotation in an oil of a chain of polystyrene spheres linked by water menisci (24). *Figure reprinted by permission from Federation Proceedings, 1967, 26:1813.*

of flexible chains of rigid spheres suspended in silicone oils with water menisci bridging the gaps between the particles (Fig. 8*C*) (24).

Rouleaux of red cells also migrate to the tube axis, at rates which are much greater than those of single red cells, an effect presumably due to the greater particle size.

Concentrated Suspensions

RED CELLS To follow individual particles in the tube flow of concentrated dispersions of 5–10% by volume is difficult, and above 10% becomes impossible because of multiple reflection and refraction of the transmitted light. In the experiments with model spherical and cylindrical particles, the problem was overcome by matching the refractive indices of suspended and suspending phases, thereby rendering the system transparent to light (25). A small quantity of particles having the same shape and size but a different refractive index were then added, and, being clearly visible, could be followed down the tube.

It is not possible to use the above technique with red blood cells. However, in this case, transparent suspensions have been prepared using human ghost cells, which after hemolysis and washing were reconstituted in biconcave form in plasma (3) at concentrations of 10–70%. About 1% by volume of the original unhemolyzed red cells was then added, and these were easily seen during flow.

The mechanics of flow of concentrated suspensions of model spheres and discs in tubes has been established in some detail (25). It is characterized, as illustrated in Fig. 9, by a particle velocity distribution or profile which is blunted from the parabolic, the velocity gradient near the wall being greater, and that in the center smaller, than in Poiseuille flow. The degree of blunting increases with increasing c and increasing ratio of particle to tube radius, b/R, but the velocity profile in a given system is independent of the flow rate. At sufficiently high c and b/R there is complete plug flow; i.e. the particles all move with the same velocity, $\bar{u} = Q/\pi R^2$. Nevertheless, these suspensions are still Newtonian in the sense that the viscosity, when measured either in tubes or in Couette viscometers, is independent of flow rate (25). The paths of individual particles in the peripheral region of the tube are erratic (Fig. 9), the spheres and discs being frequently radially displaced as a result of collisions with neighboring particles. In the center of the tube, by contrast, where G is effectively zero, their paths are undisturbed.

The behavior of human erythrocytes in ghost cell suspensions was studied over a wide range of velocities and at values of b/R ($b \sim 4\ \mu$) from 8 to 20.[1] In some respects the results paralleled those found in model rigid particle suspensions. Thus, at $c > 0.2$, the cell velocities in tubes of $R < 50\ \mu$ began to deviate from those predicted by equation 1; above $c = 0.3$, the velocity distributions were appreciably blunted, but less so than in comparable suspensions of rigid discs (Fig. 10*A*). Moreover, the deviation from the parabolic

[1] H. L. Goldsmith. Results to be published.

profile in ghost cell suspensions was somewhat greater at low flow rates than at high flow rates (Fig. 10*B*).[1]

The cells exhibited erratic radial displacements, the frequency of which decreased with decreasing r, as illustrated in Fig. 11. But most striking was their deformation into various shapes, including triangular and U-shaped

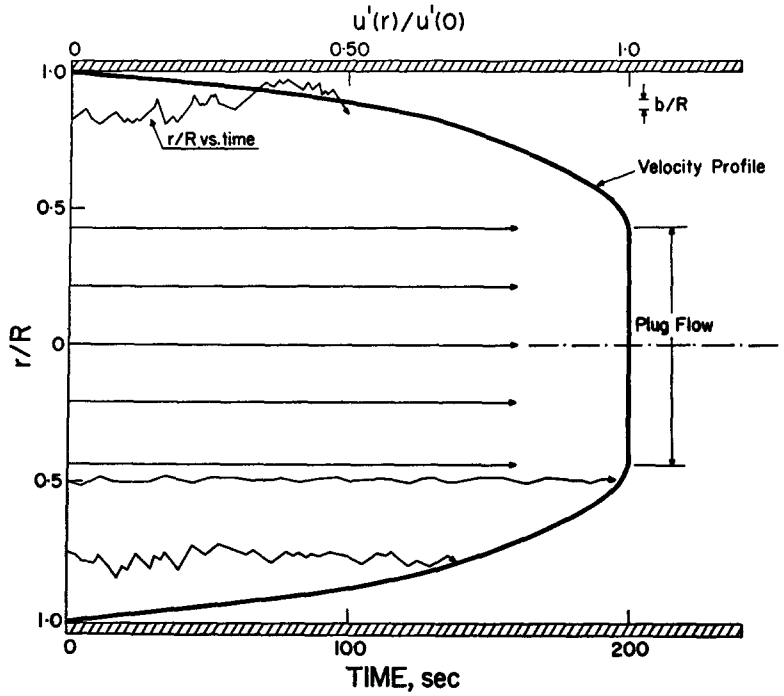

FIGURE 9. The particle velocity distribution and variation of radial distance, r, with time in a 33% suspension of model rigid spheres in tube flow at $\bar{u} = 0.08$ cm sec^{-1}. The velocities are plotted in dimensionless form, $u'(r)$ being the measured linear particle velocity, and $u'(0)$ that in the tube center (top abscissa). The distribution is markedly blunted in the center of the tube, where the particle paths (referred to the bottom time scale) are straight. In the peripheral region, however, they are erratic because of frequent collisions. The ratio $b/R = 0.016$ is shown at the top right of the graph. *Figure reprinted by permission from the Journal of Colloid and Interface Science, 1966, 22:531.*

structures, the latter like those seen in capillaries (1, 2). When red cells hardened with glutaraldehyde were followed in ghost cell suspensions, similar erratic paths were observed, but there was no cell deformation.[1]

Unlike the regular periodic rotational orbits of red cells in very dilute suspensions, the rotational motion in suspensions above $c = 0.3$ fluctuated considerably, $d\phi/dt$ being often negative. This is illustrated in Fig. 12, which compares the measured variation of the angle ϕ observed in dilute plasma

suspensions with that in a ghost cell–plasma suspension, where the ϕ-orientation is seen to fluctuate about $\phi = 0°$ (the position of alignment in the flow) while occasionally "flipping" over, rotating past $\phi = 90°$ to complete a half-orbit. As a result, the number of orbits executed by the cell in a given time was smaller than that predicted by equation 3 for $r_e = 0.40$, the effect becoming more marked at higher c. The steady-state differential distribution with respect to ϕ in a 42% ghost cell suspension is shown in the right-hand panel of

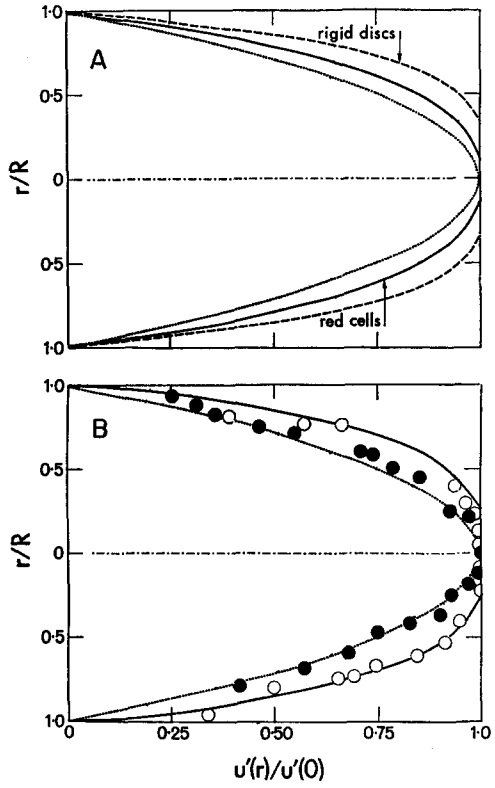

FIGURE 10. *A*. The dimensionless particle velocity distribution of human red cells in a 30% ghost cell suspension, $b/R = 0.13$ at $\bar{u} = 0.15$ cm sec^{-1}, showing slight blunting from the parabolic Poiseuille distribution (dotted line), compared with the pronounced blunting resulting in a 30% rigid disc suspension (25), $b/R = 0.08$ and $\bar{u} = 0.08$ cm sec^{-1}. The lines are the best fit of the experimental points, not shown. *B*. The change in velocity distribution of human red cells in a 64% ghost cell suspension with increasing flow rate: $\bar{u} = 0.072$ cm sec^{-1} (○) and $\bar{u} = 0.681$ cm sec^{-1} (●). The solid line is the best fit of the open circles; the dotted line is the parabolic distribution according to equation 1.

Fig. 4 and illustrates the greatly increased alignment of red cells with the flow over that existing in a dilute plasma suspension. Moreover, the degree of alignment at a given concentration increased with increasing flow rate,[1] suggesting that the cells behave partly as liquid drops, which are known to align themselves increasingly with the axial direction as the flow rate is increased (see Fig. 6) and in which the velocity gradient can be transmitted into the particle interior to produce internal circulation patterns (18, 19). The preferred orientation of erythrocytes in the direction of flow in the above experiments is in accord with measurements made in quick-frozen rabbit femoral

arteries (26) and frog mesenteric vessels (27) subsequently fixed by freeze-substitution.

ROULEAUX The above described suspensions of ghost cells in heparinized plasma differed from normal red cell suspensions in that they did not form aggregates or rouleaux when viewed under the phase contrast micro-

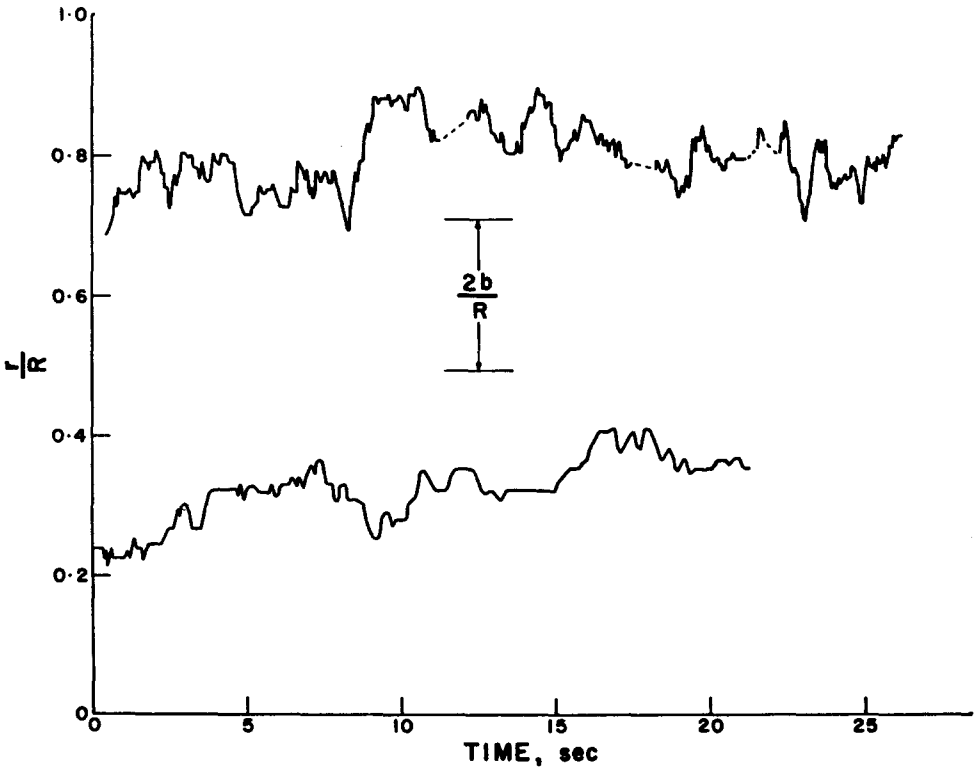

FIGURE 11. The erratic radial fluctuations of red blood cells in a transparent suspension of reconstituted ghost cells in plasma at $c = 0.42$. A plot of the dimensionless radial distance against time, showing a decrease in frequency and magnitude of particle displacements close to the tube axis, where the velocity gradient is smaller. For comparison, the diameter $2b = 8.5\ \mu$ of the red cell relative to the tube radius is also shown. *Figure reprinted by permission from Federation Proceedings, 1967, 26:1813.*

scope. Although the velocity distributions varied with the flow rate, there was not the same drastic change in flow regime which may be observed with whole blood (28), even in tubes too large to distinguish individual cell motions, except at the wall. At mean flow rates greater than 10 tube diameters/sec the blood is apparently evenly distributed across the lumen of the tube; at the wall there is a cell-depleted layer of varying thickness (3, 29) (0–8 μ), with single red cells being jostled about by collisions during the flow. However, at

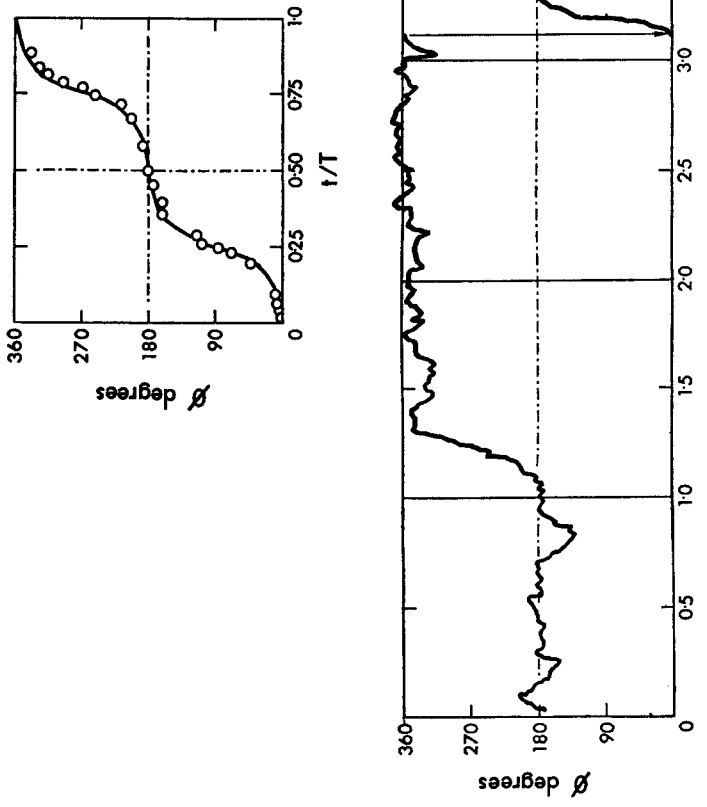

FIGURE 12. The measured variation of the ϕ-orientation of a human red cell in a 42% ghost cell suspension with time (lower) as compared with that observed at a 1% concentration in plasma (upper). In the upper part, the points are experimental and the line was calculated from equation 3 for an oblate spheroid having the equivalent axis ratio $r_e = 0.4$ obtained from the measured period of rotation, T (equation 4). In the lower part, the time has been divided into the number of orbits the cell should have executed with $r_e = 0.4$. It is evident that much time was spent by the particle in orientations close to $\phi = 180°$ and 360°, where it was aligned with the flow and, instead of 5 orbits, only 2½ were completed.

low or creeping flow rates ($\bar{u} < 2R$/sec), there is a central core having the appearance of a network of rouleaux and moving as a plug. The velocity gradient is confined to the periphery, where there is now a wider cell-depleted zone in which red cells and rouleaux may be observed to rotate and deform in the manner described above. It has also been shown (29) that in tubes where $2R = 40\ \mu$ blunting of the velocity profile at $c = 0.4$ occurs at low flow rates, the distribution in velocity becoming more parabolic as the flow rate

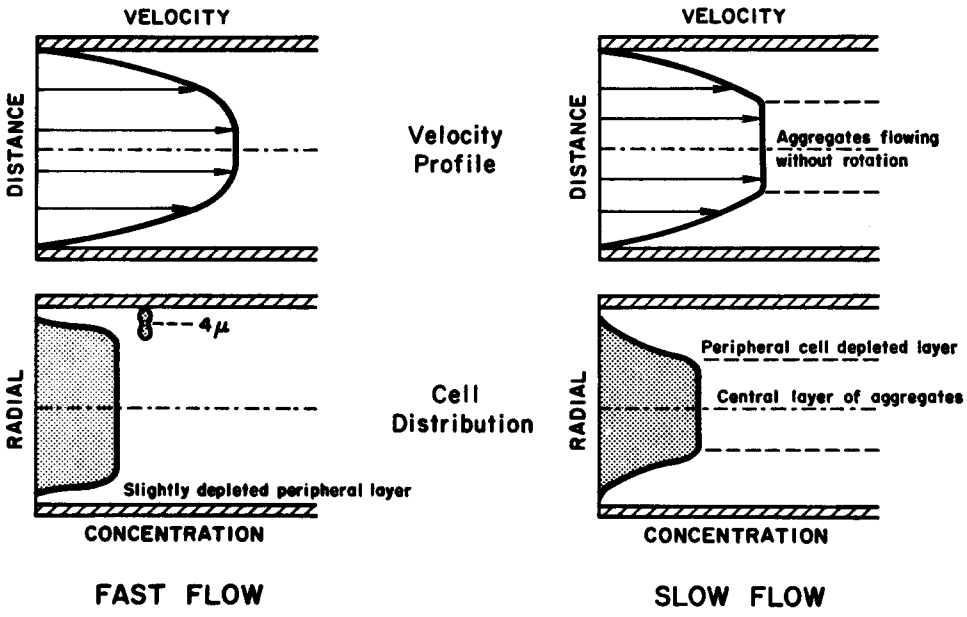

FIGURE 13. Schematic drawing of the probable velocity and particle distributions in whole blood as seen across the median plane of circular tubes at fast and low flow rates. At fast flow rates, a small degree of blunting in the velocity profile is assumed (cf. Fig. 10*B*), with a small, "particle-free" zone about 4 μ wide at the wall. At very low flow rates, the profile becomes much more blunted as a result of rouleaux formation, and this results in the formation of a much wider particle-free zone at the wall.

increases. The difference in velocity and particle distribution in the two flow regimes is schematically portrayed in Fig. 13.

Such an obvious change in velocity profile is not observed in concentrated suspensions of erythrocytes in Ringer's solution (30), where rouleaux do not form and where, in a Couette viscometer, erythrocytes exhibit Newtonian behavior at all velocity gradients.

AXIAL MIGRATION There is quantitative evidence that a fluctuating red cell–depleted layer up to 8 μ in thickness exists at the wall of arterial vessels of diameter up to 0.1 cm (26, 27). That inward migration of erythrocytes does

not proceed further is not surprising, since the concentration in the vessels is so high. However, model experiments with rigid spheres in both steady (31) and pulsatile flow (32) indicate that inward migration [here due to inertial effects (9)], even when limited to one or two particle diameters from the wall and continually fluctuating in width, can lead to a significant reduction in the energy dissipation in the flow (32). This is probably due to the establishment of a two-phase flow of a central core containing the particles, surrounded by a peripheral, particle-depleted layer of relatively lower viscosity.

TUBES OF THE SAME SIZE AS RED CELLS

Flow Pattern: Bolus Flow

The vessels of the capillary bed are comparable in diameter to the red cells, and often are even smaller. The effect on the undisturbed Poiseuille flow by a particle under these conditions must be quite different from that which prevails in tubes many times the particle diameter. In the simple case of a rigid sphere in a sheared fluid, the disturbance to the flow, as illustrated by the disturbance to the fluid streamlines around the particle shown in Fig. 14, can be seen to have virtually died out at 1.5 sphere diameters from its center. The disturbance is even smaller in the case of a fluid drop, where the velocity gradient is transmitted into the particle interior (18). If the particle is much smaller than the tube, the situation, in the absence of particle-particle interaction, is not much different from that of the undisturbed suspending fluid undergoing Poiseuille flow. But when $b/R > 0.5$, the effect of the particle is pronounced, and in the limiting case of a train of particles following one another down the tube the flow has been termed bolus flow (33) when the suspended phase consists of large liquid or gaseous bubbles (Fig. 15, top left). Bolus flow of liquid, neutrally buoyant bubbles is characterized by the fact that (*a*) the bubbles are of cylindrical shape and flow axisymmetrically down the tube, surrounded by a layer of suspending phase liquid of constant thickness between the front and rear end curvatures of the bubble (34), and (*b*) in an axial core of the liquid between the rear end of one bubble and the leading end of the next, circulation patterns are set up. The effect of such flow is that a bolus of suspending liquid between the bubbles is carried down the tube with the bubble velocity, while a layer of liquid at the tube wall is bypassed. The volume of liquid bypassed depends on the thickness of the layer surrounding the bubble; at low flow rates, this increases with the square root of the bubble velocity (34).

The velocity profiles in the bubble and surrounding liquid depend on the value of λ (viscosity of bubble phase/viscosity of suspending phase). When the bubble has negligible viscosity compared to the suspending liquid, there is no flow in the film (34). The ratio of the pressure drop across the bubble

ends to the pressure drop across an equal length of pure suspending fluid, the "bubble resistance factor," has been shown for short bubbles (length/tube diameter = 2–4) in systems of $\lambda = 0$ to be only slightly greater than unity (35). In this case the additional pressure drop due to the presence of the bubble arises from effects associated with the bubble ends.

When $\lambda > 0$, velocity gradients develop in the film (Fig. 15, center) and internal circulation can be seen inside the bubble, showing that the gradient has been transmitted across the interface. As λ increases, the gradients in the

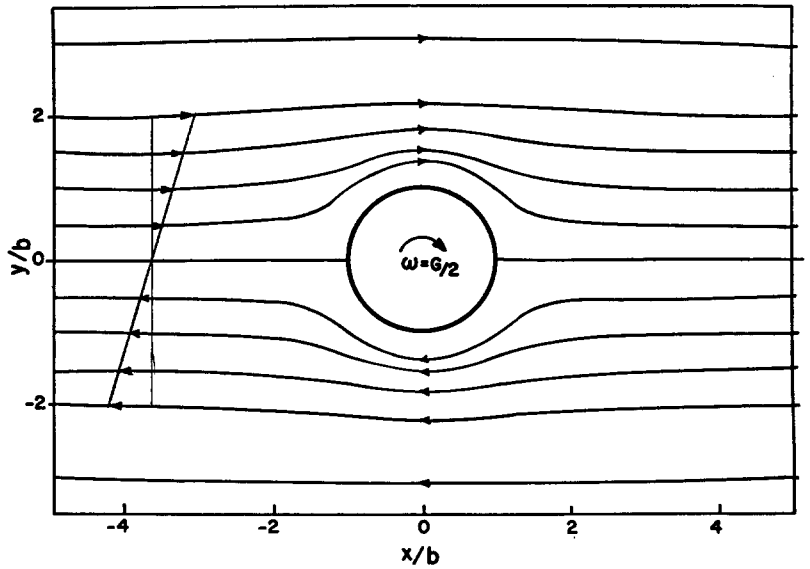

FIGURE 14. The disturbance created by a rigid sphere rotating with constant angular velocity, $G/2$, in a liquid subjected to a simple shear flow. The sphere is shown at the origin of the flow field, and the fluid streamlines around it are plotted in units of sphere radii in the y and x directions. *Figure reprinted by permission from the Journal of Colloid Science, 1958, 13:293.*

film increase, and those in the bubble decrease until, at high λ, the system approaches plug flow. In this case the bubble resistance factor may have values as high as 10–20 (36), and in a system where a train of bubbles travels down a tube a large increase in the pressure gradient at a given flow rate would be expected.

It is interesting, therefore, that the measured apparent viscosity of blood in tiny glass capillaries having a tip of 5 μ bore is only 5% greater than that of plasma (37). Further work will be necessary before the significance of this result in terms of the red cell and internal circulation is understood.

However, it is evident that the mixing or vortex motion in the bolus of fluid carried between cells may be important as an aid to the exchange and

diffusion of substances between the vascular and extravascular compartments. Model experiments with a train of gas bubbles at high flow rates using a thermal analogue (33) showed that the heat transfer in bolus flow is approximately twice that in Poiseuille flow for the same volume of fluid. The difference decreased with decreasing flow rate, tending to zero at zero flow rate.

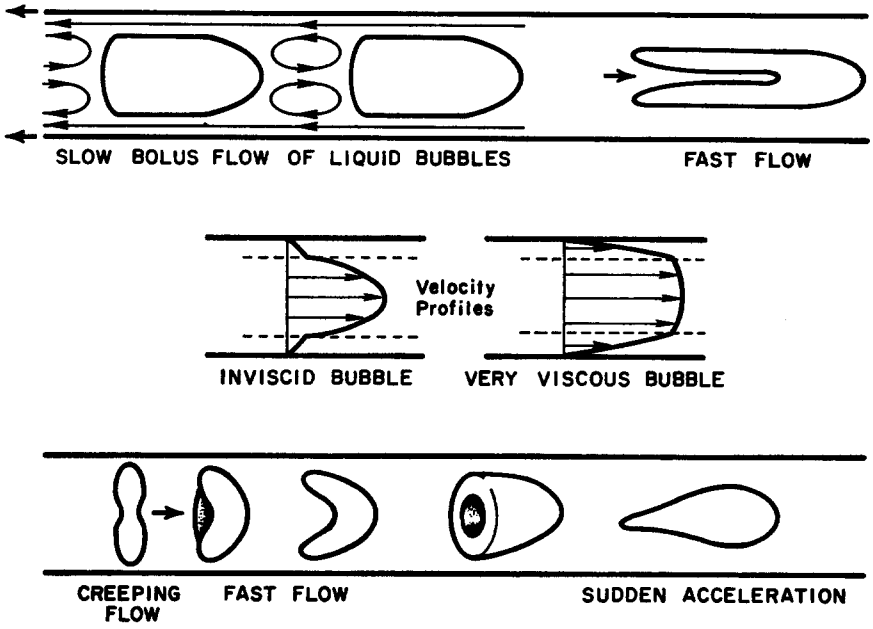

FIGURE 15. Flow and deformation in systems where the particle is of the same size as the vessel. The upper part shows the bolus flow of a train of liquid bubbles flowing axisymmetrically in the tube surrounded by a layer of suspending liquid. The tube has been moved back with the velocity of the bubble so as to render the particle stationary. The center part shows the velocity profiles which have been measured in the liquid layer and the bubble as a function of the bubble/suspending liquid viscosity ratio (34). The dashed line represents the position of the interface. At top right, the reentrant cavity which develops upon fast flow of the bubbles is shown; this is similar to the shapes seen in red cells in the capillaries of the circulation illustrated in the bottom part.[2]

Deformation

Visual studies of the capillary bed have shown that flow is intermittent (38–40) and that groups of erythrocytes often pass through separated by plasma. With the use of improved optical techniques and high-speed cinemicrography (1, 2, 41), the flow behavior of the individual cells has been observed. At zero flow they are seen edge on, with their faces most often oriented perpendicular to the vessel. As flow increases, deformation sets in and the erythrocytes become U-shaped, thimble-shaped, and teardrop-shaped. Such deformation,

[2] H. L. Goldsmith. Unpublished observations.

illustrated at the bottom of Fig. 15, has also been seen in glass capillaries of 8–10 μ diameter.[2] The preferred broad-side-on orientation of the red cells appears to be a more general phenomenon, since it has been observed also with model plane and biconcave discs in tubes where $b/R > 0.8$ (42).

A similar type of deformation has been seen with liquid bubbles in tube flow (34). At low flow rates, the bubbles are bullet-shaped, as shown in Fig. 15. As the volume flow rate increases, the leading end becomes more elliptical and the trailing end develops a reentrant cavity (Fig. 15, top right) of suspending phase liquid whose volume increases with time and, as it penetrates the bubble, is pulled out into a thread of liquid which travels the length of the bubble.

Finally, it should be pointed out that bolus flow in the capillary provides a mechanism for flow-dependent red cell–plasma separation in transit through the bed. It arises from the greater linear flow velocity of the cells over the mean velocity of the plasma. Since the deformation of the cells at higher flow rates can visually be seen to result in their elongation and thinning, one would assume that they then bypass more plasma during flow, resulting in a larger difference between mean red cell and plasma transit times.

The author wishes to thank Mrs. M. Pitteway for her technical assistance.
This investigation was supported by research grant MT-1835 from the Medical Research Council of Canada.

REFERENCES

1. BRÄNEMARK, P.-I., and J. LINDSTRÖM. 1963. Shape of circulating blood corpuscles. *Biorheology*. **1**:139.
2. GUEST, M. M., T. P. BOND, R. G. COOPER, and J. R. DERRICK. 1963. Red blood cells: change in shape in capillaries. *Science*. **142**:1319.
3. GOLDSMITH, H. L. 1967. Microscopic flow properties of red cells. *Federation Proc.* **26**:1813.
4. BAYLISS, L. E. 1952. Rheology of blood and lymph. *In* Deformation and Flow in Biological Systems. A. Frey-Wyssling, editor. North Holland Publishing Company, New York. 398.
5. BRODNYAN, J. G., and E. L. KELLEY. 1965. The effect of electrolyte content on synthetic latex flow behavior. *J. Colloid Sci.* **20**:7.
6. TAYLOR, H. M., S. CHIEN, and M. I. GREGERSON. 1965. Comparison of viscometric behavior of suspensions of polystyrene latex and human blood cells. *Nature*. **207**:77.
7. RICHARDSON, E. G. 1950. The formation and flow of emulsions. *J. Colloid Sci.* **5**:404.
8. HARRIS, J. W., H. A. BREWSTER, T. H. HAM, and W. B. CASTLE. 1956. Studies on the destruction of red blood cells. X. The biophysics and biology of sickle-cell disease. *A.M.A. Arch. Internal Med.* **97**:145.
9. GOLDSMITH, H. L., and S. G. MASON. 1967. The microrheology of dispersions. *In* Rheology: Theory and Applications. IV. F. R. Eirich, editor. Academic Press, Inc., New York. 86.
10. MÜLLER, A. 1936. Abhandlungen zur Mechanik der Flüssigkeiten. University of Fribourg, Fribourg, Switzerland. I.
11. DINTENFASS, L. 1964. Rheology of packed red blood cells containing hemoglobins A-A, S-A and S-S. *J. Lab. Clin. Med.* **64**:594.
12. KURODA, K., Y. MISHIRO, and I. WADA. 1958. Relation between the viscosity of erythrocyte suspensions and the shape of the erythrocyte. *Tokushima J. Exptl. Med.* **4**:73.

13. CHIEN, S., S. USAMI, R. J. DELLENBACK, and M. I. GREGERSON. 1967. Blood viscosity: influence of erythrocyte deformation. *Science.* **157**:287.
14. JEFFERY, G. B. 1922. On the motion of ellipsoidal particles immersed in a viscous fluid. *Proc. Roy. Soc. (London), Ser. A.* **102**:162.
15. GOLDSMITH, H. L., and S. G. MASON. 1962. The flow of suspensions through tubes. I. Single spheres, rods and discs. *J. Colloid Sci.* **17**:448.
16. GOLDSMITH, H. L. 1966. Red cells and rouleaux in shear flow. *Science.* **153**:1406.
17. MASON, S. G., and R. ST. J. MANLEY. 1956. Particle motions in sheared suspensions. IV. Orientations and interactions of rigid rods. *Proc. Roy. Soc. (London), Ser. A.* **238**:117.
18. BARTOK, W., and S. G. MASON. 1958. Particle motions in sheared suspensions. VII. Internal circulation in fluid droplets (theoretical). *J. Colloid Sci.* **13**:293.
19. RUMSCHEIDT, F. D., and S. G. MASON. 1961. Particle motions in sheared suspensions. XI. Internal circulation in fluid drops (experimental). *J. Colloid Sci.* **16**:210.
20. TAYLOR, G. I. 1934. The formation of emulsions in definable fields of flow. *Proc. Roy. Soc. (London), Ser. A.* **146**:501.
21. RUMSCHEIDT, F. D., and S. G. MASON. 1960. Particle motions in sheared suspensions. XII. Deformation and burst of fluid drops in shear and hyperbolic flow. *J. Colloid Sci.* **16**:238.
22. CHAFFEY, C. E., H. BRENNER and S. G. MASON. 1965. Particle motions in sheared suspensions. XVIII. Wall migration (theoretical). *Rheol. Acta.* **4**:64.
23. FORGACS, O. L., and S. G. MASON. 1959. Particle motions in sheared suspensions. IX. Spin and deformation of thread like particles. *J. Colloid Sci.* **14**:457.
24. ZIA, I. Y., R. G. COX, and S. G. MASON. 1966. Chains of particles in shear flow. *Science.* **153**:1405.
25. KARNIS, A., H. L. GOLDSMITH, and S. G. MASON. 1966. The kinetics of flowing dispersions. I. Concentrated suspensions of rigid particles. *J. Colloid Interface Sci.* **22**:531.
26. PHIBBS, R. H. Orientation and distribution of erythrocytes in blood flowing through medium-sized arteries. *In* Proceedings of the First International Congress on Hemorheology. A. L. Copley, editor. Pergamon Press, New York. In press.
27. WIEDERHIELM, A., and L. BILLIG. Effects of erythrocyte orientation and concentration on light transmission through blood flowing through microscopic blood vessels. *In* Proceedings of the First International Congress on Hemorheology. A. L. Copley, editor. Pergamon Press, New York. In press.
28. BENIS, A. M. 1964. The flow of blood through models of the microcirculation. Doctorate Thesis. Massachusetts Institute of Technology, Cambridge.
29. BUGLIARELLO, G., C. KAPUR, and G. HSIAO. 1965. The profile viscosity and other characteristics of blood flow in a non-uniform shear field. *Proc. Intern. Congr. Rheol., 4th, Providence, R.I.* Interscience Publishers, Inc., New York. 351.
30. MERRILL, E. W., A. M. BENIS, E. R. GILLILAND, T. K. SHERWOOD, and E. W. SALZMAN. 1965. Pressure-flow relations in human blood in hollow fibers at low flow rates. *J. Appl. Physiol.* **20**:954.
31. KARNIS, A., H. L. GOLDSMITH, and S. G. MASON. 1966. The flow of suspensions through tubes. V. Inertial effects. *Can. J. Chem. Eng.* **44**:181.
32. TAKANO, M., H. L. GOLDSMITH, and S. G. MASON. 1968. The flow of suspensions through tubes. IX. Particle interactions in pulsatile flow. *J. Colloid Interface Sci.* **24**.
33. PROTHERO, J. W., and A. C. BURTON. 1961. The physics of blood flow in capillaries. I. The nature of the motion. *Biophys. J.* **1**:565.
34. GOLDSMITH, H. L., and S. G. MASON. 1963. The flow of suspensions through tubes. II. Single large bubbles. *J. Colloid Sci.* **18**:237.
35. GOLDSMITH, H. L. 1961. The microrheology of suspensions. Doctorate Thesis. McGill University, Montreal.
36. MARCHESSAULT, R. H., and S. G. MASON. 1960. Flow of entrapped bubbles through a capillary. *Ind. Eng. Chem.* **52**:79.
37. PROTHERO, J. W., and A. C. BURTON. 1961. The physics of blood flow in the capillaries. II. The capillary resistance to flow. *Biophys. J.* **2**:199.

38. PALMER, A. A. 1959. A study of blood flow in minute vessels of the pancreatic region of the rat with reference to intermittent corpuscular flow in individual capillaries. *Quart. J. Exptl. Physiol.* **44**:149.
39. MONRO, P. A. G. 1964. The appearance of cell-free plasma and grouping of cells in normal circulation in small blood vessels observed *in vivo*. *Biorheology*. **1**:239.
40. JOHNSON, P. C., and H. WAYLAND. 1967. Regulation of blood flow in single capillaries. *Am. J. Physiol.* **212**:1405.
41. BLOCH, E. H. 1962. A quantitative study of the hemodynamics of the living microvascular system. *Am. J. Anat.* **110**:125.
42. SUTERA, S. P., and R. M. HOCHMUTH. 1968. Large scale modelling of blood flow in the capillaries. *Biorheology*. **5**: 45.

Discussion

Question from the floor: Could you tell us the size of the tubes and of the spheres in the last sequence of the movie in which you showed bolus flow?

Dr. Goldsmith: Two polystyrene spheres approximately 1.8 mm in diameter were suspended in a viscous oil of the same density moving through a tube 2.0 mm in diameter at 1 mm/sec. The spheres were separated by a distance of about 3–4 mm and were followed down the tube with a traveling microscope. The liquid contained aluminium tracer particles, which acted as markers for the streamlines.

Dr. Roe Wells: Because of the importance of the dynamics on that very first slide, the influence of rigidity vs. fluidity of the drop in various media, I was wondering if you had studied a concentrated suspension of your clear plastic model system, since this would permit some light transmission and enable you to evaluate the effects of rigidity vs. plasticity in such a system. Also, have you had occasion to take your excellent ghost study system and embalm it, say with one of the aldehydes, to study the effect of rigidity after the fact? I think both of these would underscore the question of this fluidity concept, which is so important.

Dr. Goldsmith: As I mentioned in my talk, we have studied the flow of concentrated suspensions in the clear rigid plastic sphere system. As shown in Fig. 9, the influence of rigidity is felt by a much greater blunting of the velocity profile. Unlike the ghost cell deformable system, the velocity distribution in the center of the tube is flat; i.e. there is plug flow in this region.

In answer to the second part of your question, we have not yet transformed the ghost cell system although we intend to do this. What we have done is to observe glutaraldehyde-hardened red cells *in* the ghost system. This, of course, does not change the velocity profile or the radial variation in cell paths with time, because 99 % of the system still consists of pliable ghost cells. But here, the hardened cells do not deform during travel and behave as rigid bodies. We do know, however, that a suspension of glutaraldehyde-hardened red cells has a viscosity an order of magnitude higher than that of red cells.

Dr. Lysle H. Peterson: I wonder if you would comment, from your excellent studies, on the effects which tend to turbulence. As I understand it, much of your studies has been concerned with established flow. Would you comment on cell distribution in three conditions which, for example, cause turbulence? One is bending of the tube, the other one is in tapering, in which the radius varies, and the third is with cell suspensions at higher velocities.

Dr. Goldsmith: You wish me to comment on the effects of turbulence in such systems?

Dr. Peterson: Yes, the effects of tube bending, the effects of tube tapering, and the effects of higher Reynolds numbers.

Dr. Goldsmith: My present studies really have very little bearing on your question. As regards flow at bends or bifurcations, it is well known that one can get flow separation from the wall with the attendant formation of vortices. This may be of importance in the studies of the formation of atherosclerotic plaques, since it has been postulated that, at sufficiently high velocities of flow, platelets will get trapped in these vortices and may collide with the wall and each other. This could lead to the formation of emboli. We haven't studied such flows. About the other two situations I cannot comment.